

## Optical properties study of PMMA/PbO (NPs) composites films

Sarah A.Elawam<sup>1</sup>, Wafaa M.Morsi<sup>2</sup>, Hoda M.Abou-Shady<sup>3</sup>, Osiris W.Guirguis<sup>1\*</sup>

<sup>1</sup>Biophysics Department, Faculty of Science, Cairo University, Giza (EGYPT)

<sup>2</sup>Building Physics Institute, Housing and Building National Research Center (HBRC), Giza, (EGYPT)

<sup>3</sup>Physics Department, Faculty of Science, Cairo University, Giza (EGYPT)

E-mail: osiris\_wgr@yahoo.com

### ABSTRACT

In the present work, thin films of poly(methyl methacrylate)/lead oxide nanoparticles composites [PMMA/PbO(NPs)] were prepared using solution-cast method. The effect of PbO NPs with different concentrations in the range from 0.26 to 1.00 wt% on the transmittance spectra in the spectral region 400-700 nm was followed using spectrophotometer tool, CIE tristimulus values and color parameters. The changes in the optical parameters including: absorption coefficient, band tail width and band gap energies, extinction coefficient and color strength as well as refractive index and dispersion parameters were investigated. The data obtained indicated that the optical parameters were highly affected by changing PbO NPs concentration. The dispersion parameters were changed by incorporation of PbO. In conclusion, the obtained optical parameters of PMMA were found to be strongly affected its optical properties by addition of PbO nanoparticles. © 2016 Trade Science Inc. - INDIA

### KEYWORDS

Poly(methyl methacrylate);  
Lead oxide nanoparticles;  
Optical parameters;  
Tristimulus values;  
Color parameters;  
Refractive index;  
Optical dispersion.

### INTRODUCTION

According to the physical and chemical properties and applications in different medical and industrial fields, nano-materials were attracted the interesting of many investigators<sup>[1,2]</sup>. On other hand, nano-materials have a long axis to absorb incident sunlight, one-dimensional nanostructures were gained attention in solar energy conversion<sup>[3,4]</sup>.

Lead oxides (PbO) are fascinating compounds because of their four numerous phases: PbO ( $\alpha$ ,  $\beta$  and amorphous), Pb<sub>2</sub>O<sub>3</sub>, Pb<sub>3</sub>O<sub>4</sub>, PbO<sub>2</sub> ( $\alpha$ ,  $\beta$  and amorphous)<sup>[5-7]</sup>. PbO has two polymorphic forms: a red  $\alpha$ -PbO, which is stable at low temperature and a

yellow  $\beta$ -PbO, which is stable at temperatures higher than 425 °C. PbO has a wide band gap and a high refractive index. A mixture of  $\alpha$ - and  $\beta$ -PbO nanocrystals could be obtained via the calculation of both lead citrate and lead oxalate<sup>[8]</sup>. Moreover, lead oxide nanoparticles [PbO(NPs)] were used in medical, pharmaceutical, nuclear and space industries applications such as; gamma ray protective clothing, shielding, magnetic imaging, batteries, X-ray sensing application and drug delivery as well as they have antibacterial uses<sup>[9-13]</sup>. PbO nanostructure could be synthesized using various methods<sup>[5,14]</sup>. The sol-gel method shows considerable advantages over the customary methods and provides a low cost, simple,

## Full Paper

non-hazardous technique for the preparation of different nano-oxides.

Polymers have special interest they give complexes when they were in combination with suitable metal salts. These complexes were useful for the development of photo-electrochemical cells and advanced high energy electrochemical devices with ease of fabrication into thin films. Also polymer-inorganic oxide nanoparticles composites have attracted interest in the field of material science due to they exhibit enhanced material properties in comparison with the pure polymers. Now, composites make of polymers and nanoparticles such as; inorganic, metal, semiconductor, carbon black, and magnetic nanomaterials have attracted great attention because of the stabilizing effects of the polymer matrix on the nanoparticles<sup>[15,19]</sup>.

Poly(methyl methacrylate (PMMA) has various applications in many technological and productive fields. It is an important thermoplastic material. PMMA takes advantages of the unique combination of excellent optical properties (transparency in a wide range from the near ultraviolet to the near infrared). In addition, PMMA is very suitable for numerous imaging and non-imaging microelectronic applications such as a photoresistance for direct-write e-beams, X-rays and deep UV microlithographic process. It has been used to make a variety of optical devices such as optical lenses<sup>[20,21]</sup>. PMMA has thermal stability, electrical properties, safety, weather resistance, model ability and easy shaping<sup>[22]</sup>. PMMA was also used in skeletal surgery as a means of securing prosthetic implants and as a delivery agent for local high-dose antibiotics to treat soft tissue, extremely utilized for antibiotic delivery system purposes for the treatment of osteomyelitis and osseous infections<sup>[23,24]</sup>. In addition, PMMA is a widely used support medium for the embedding of intact, undecalcified bone<sup>[25]</sup> and its hardness makes it ideal for calcified tissue sectioning and subsequent histological examination<sup>[26]</sup>.

The objective of the present study is to prepare thin films of PMMA/PbO(NPs) composites. The influence of PbO NPs with different concentrations on the optical properties of the prepared films was investigated.

## EXPERIMENTAL

### Materials and sample preparation

In the present work, lead diacetate of chemical formula  $[\text{Pb}(\text{CH}_3\text{COO})_2]$  with average molecular weight 279.33 and oxalic acid  $[\text{C}_2\text{H}_2\text{O}_4]$  of molecular weight 126.07, supplied from Adwik, Egypt, were used. Poly(methyl methacrylate) powder of chemical formula  $[\text{CH}_2\text{C}(\text{CH}_3)(\text{CO}_2\text{CH}_3)_n]$  with average molecular weight 320,000 was supplied from Alfa Aesar, GmbH & Co., KG.

The sol-gel process was used to get lead oxide nanoparticles  $[\text{PbO}(\text{NPs})]$ <sup>[27-29]</sup>. In this method, weighted amounts of lead diacetate and oxalic acid were dissolved in 200 mL double distilled water under a magnetic stirring for about 1 h at 60 °C to give a white colloidal suspension. The obtained sol was kept in an electrical oven at about 80 °C for 8 h, cooled gradually to room temperature (about 25 °C) and stirred to get the gel form. The gel was aged for 18 h at about 25 °C. The obtained gel was calcined at about 900 °C for 1 h to give yellow-greenish PbO nano-powders. The X-ray diffraction (XRD) pattern (data not shown) indicates that the obtained PbO nano-powder was a mixture of orthorhombic  $\beta$ -PbO and tetragonal  $\alpha$ -PbO phases and the average crystalline size was found to be about 84 nm.

The prepared PbO(NPs) were added in different ratios,  $x$  (0, 0.26, 0.48, 0.52, 0.78 and 1.00 wt%) to PMMA by using the relation<sup>[29]</sup>:

$$x = \left[ \frac{W_f}{(W_f + W_p)} \right] \times 100 \quad (1)$$

$W_f$  is the weight of PbO(NPs) and  $W_p$  is the weight of PMMA. Five thin films of PMMA/PbO(NPs) composites (100.00/0.00, 99.74/0.26, 99.48/0.52, 99.22/0.78 and 99.00/1.00 wt/wt%) were prepared by casting method as follows<sup>[27-29]</sup>: a weight amount of PMMA was dissolved in toluene (70 ml) with stirring for 1 h at 60 °C until the polymer completely dissolved. PbO(NPs) were added to the PMMA solution in the appropriate ratio under vigorous stirring to prevent agglomeration. Finally, the solution were cast into stainless steel Petri dishes and placed in an oven at 60 °C for 24 h in air. Care was taken to obtain films of uniform thickness ( $H''$  0.01 mm) for recording optical transmittance spectra. The samples were measured at room tempera-

ture as solid films (slabs) of dimensions 1 x 4 cm.

### Optical measurements

The optical transmittance for the prepared PMMA/PbO(NPs) composites films were recorded in the visible range from 400 to 700 nm by using a Shimadzu UV/VIS/NIR Double Beam Spectrophotometer (Japan) with standard illuminant C (1174.83), model V-530 and band width 2.0 nm covers the range 200-2500 nm with accuracy  $\pm 0.05\%$ . The color properties were analyzed using the CIE Colorimetric System, CIE 1931 2-degree Standard Observer<sup>[30,31]</sup>. The tristimulus transmittance values

( $x_r$ ,  $y_r$  and  $z_r$ ), the relative brightness (L), the color constants 'a' and 'b', the whiteness index (W), the color difference ( $\Delta E$ ), the chroma ( $\Delta C$ ) and the hue ( $\Delta H$ ) were calculated using the CIE relations previously reported<sup>[32]</sup>.

The recorded data for each composite were an average of three measurements taken from three slabs from the same film.

## RESULTS AND DISCUSSIONS

Figure 1 shows the transmittance spectra of

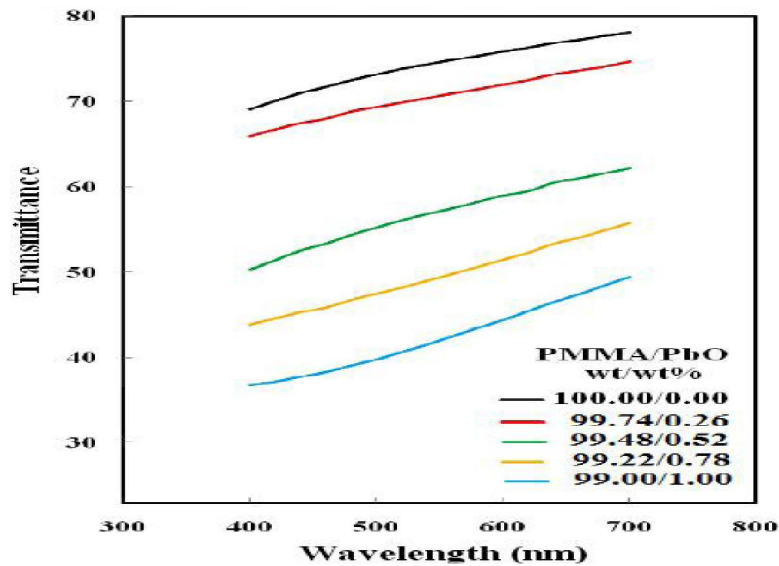


Figure 1 : The transmittance spectra of PMMA/PbO(NPS) composites

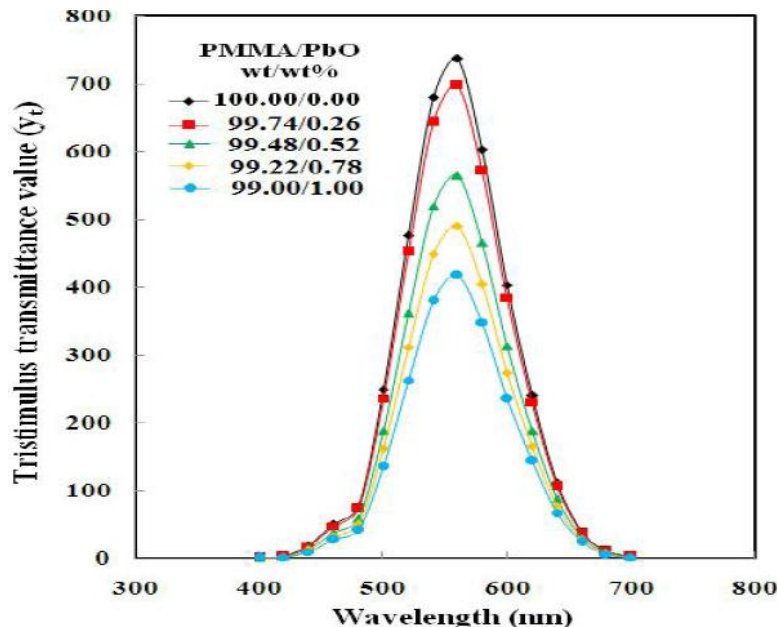


Figure 2 : Variation of the tristimulus transmittance value ( $y_r$ ) with wavelength for PMMA/PbO(NPS) composites

## Full Paper

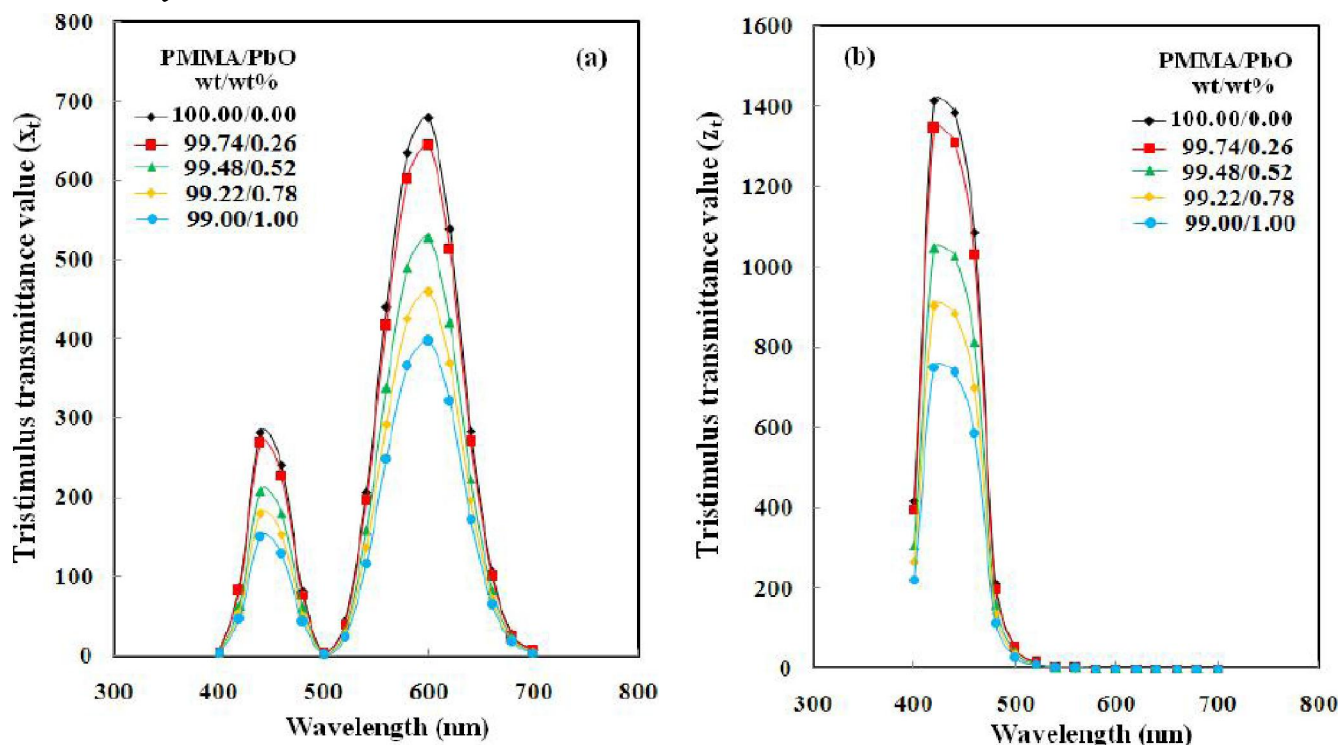


Figure 3 : Variations of the tristimulus transmittance value,  $x_r$  (a) and tristimulus transmittance value,  $z_r$  (b) with wavelength for PMMA/PbO(NPS) composites

PMMA/PbO(NPS) composites in the wavelength range 400-700 nm. It is clear from the figure that there is an observable decrease in the transmittance value for the whole spectrum of the composite with increasing the concentration of PbO NPs up to 1.00 wt%. This variation in the transmittance values may be attributed to the fact that increasing PbO NPs concentration decreases the transparency of the sample which may be due to that there is a change in the molecular configuration<sup>[33,34]</sup>.

From the transmittance values (Figure 1), the tristimulus transmittance values ( $y_r$ ) of PMMA/PbO(NPS) composites were calculated and plotted as a function of wavelength (400-700 nm) and shown in Figure 2. It is observed that, the behaviors of  $y_r$  for the composites are similar and there is no change in the peak position (at 560 nm). It is also observed that,  $y_r$  value decreases with increasing PbO NPs up to 1.00 wt%.

Figure 3a and Figure 3b show the variations of the tristimulus transmittance values ( $x_r$ ) and ( $z_r$ ), respectively, with wavelength. It is clear that the behaviors of the samples are similar and show the same peak positions. Also,  $x_r$  and  $z_r$  values decrease with

increasing PbO NPs up to 1.00 wt%.

TABLE 1 illustrates the values of  $x_r$ ,  $y_r$  and  $z_r$  at their peak positions and TABLE 2 represents the percentage changes in the maximum tristimulus transmittance values for PMMA/PbO(NPS) at their band positions.

From the obtained data, the observed variations may be attributed to that there is a change in the molecular configuration which indicates to the formation of new color centers<sup>[33,34]</sup>.

TABLE 3 represents the variations of color parameters such as; brightness (L), color constants, 'a' and 'b' and whiteness index (W) calculated from the transmittance values (Figure 1) and their percentage changes for PMMA/PbO(NPS) composites. From the table it is noticed that: The relative brightness (L) shows decrease in their values with increasing the concentration of PbO NPs which means that the composites become fader in color. The values of the color constant 'a' increase by increasing the PbO NPs content up to 1.00 wt% which indicates that, there is an increase in red component instead of green one. The values of the color constant 'b', also, increase by increasing PbO NPs which indicates that

**TABLE 1 :** The maximum tristimulus transmittance values ( $x_r$ ,  $y_r$  and  $z_r$ ) for PMMA/PbO(NPS) composites at their peak positions

PMMA/PbO(NPS) composite (wt/wt%)	$x_r$		$y_r$	$z_r$
	$\lambda = 440 \text{ nm}$	$\lambda = 600 \text{ nm}$	$\lambda = 560 \text{ nm}$	$\lambda = 440 \text{ nm}$
100.00/0.00	282.225	678.692	736.796	1415.598
99.74/0.26	268.193	643.881	697.825	1345.217
99.48/0.52	208.608	527.544	565.267	1046.346
99.22/0.78	179.869	460.247	489.688	902.195
99.00/1.00	149.778	396.888	417.455	751.264

**TABLE 2 :** The percentage changes in the maximum tristimulus transmittance values for PMMA/PbO(NPS) at their band positions

PMMA/PbO(NPS) composite (wt/wt%)	$(\Delta x_r)\%$		$(\Delta y_r)\%$	$(\Delta z_r)\%$
	$\lambda = 440 \text{ nm}$	$\lambda = 600 \text{ nm}$	$\lambda = 560 \text{ nm}$	$\lambda = 440 \text{ nm}$
100.00/0.00	-	-	-	-
99.74/0.26	4.97	5.13	5.29	4.97
99.48/0.52	26.08	22.27	23.28	26.08
99.22/0.78	36.28	32.19	33.54	36.28
99.00/1.00	46.93	41.52	43.34	46.93

there in an increase in yellow component instead of blue one. Opposite behavior is observed for the whiteness index (W) in comparison with the color constants 'a' and 'b'. The observed decrease in the whiteness index (W) values and the results of the color scales ( $\Delta E$ ,  $\Delta C$  and  $\Delta H$ ) indicate that variations in color difference between the composites were occurred due to the presence of different concentrations of PbO NPs with PMMA.

The remarkable variations in the color parameters calculated from the transmittance spectra with increasing the concentration of PbO NPs may be attributed to change in physical bonds and then changes in the molecular configuration of PMMA were occurred as mentioned before<sup>[33,34]</sup>. These variations in the molecular configuration may lead to formation of new dopant centers of the polymeric material. Furthermore, the obtained data of the color parameters are of great importance for the improvement of the optical properties of the PMMA.

From the optical transmittance spectra, the absorption coefficient ( $\alpha$ ) of the prepared composites films was calculated using the following relation<sup>[32,35,36]</sup>:

$$\alpha = (1/d) [\ln (1-R)^2/T] \quad (2)$$

where d is the thickness of the sample in cm, T is the

transmittance value and R is the reflectance value. The absorption coefficient values ( $\alpha$ ) for the prepared films were calculated in the visible wavelength range 400-700 nm and in the photon energy range 1.77-3.10 eV. Figure 4 shows the variation between the absorption coefficient ( $\alpha$ ) as a function of wavelength (a) and photon energy, hv (b) for PMMA/PbO(NPS) composites. It is clear from the figure that,  $\alpha$  values increases with increasing PbO NPs content up to 1.00 wt%. This may be attributed to the changes of the molecular configuration which indicates to the formation of new color centers<sup>[32,33,35]</sup>. TABLE 4 illustrates values of absorption coefficient ( $\alpha$ ) and their percentage changes at 560 nm.

For amorphous materials, an exponential dependence on photon energy (hv) in the low absorption region of the absorption coefficient ( $\alpha$ ) was shown and obeys Urbach relation<sup>[32,35-37]</sup>:

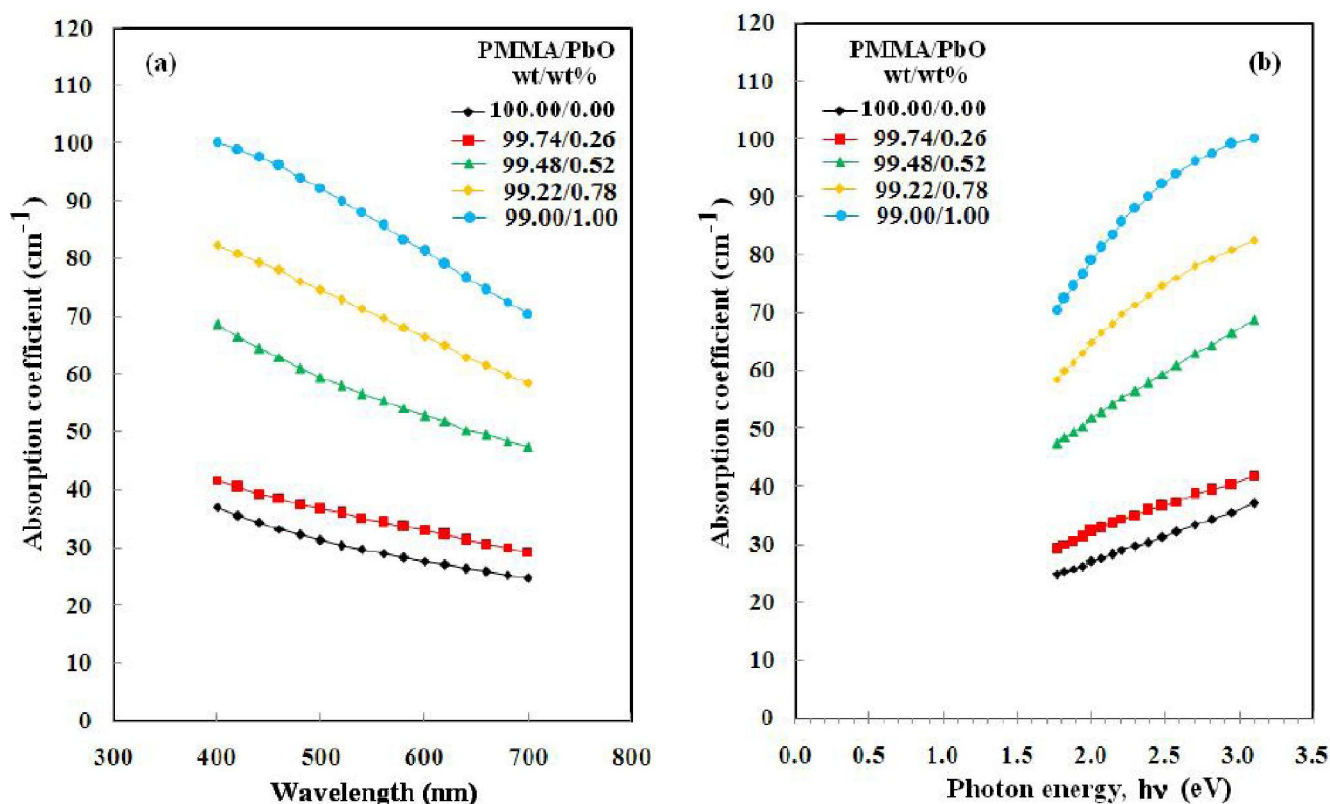
$$\alpha = \alpha_0 \exp (hv/E_b) \quad (3)$$

where  $\alpha_0$  is a constant,  $\nu$  is the frequency of radiation and  $E_b$  is the energy which interpreted the width of the tail localized states in the normally forbidden band gap and associated with the amorphous nature of the polymeric materials. The relation between  $-\ln \alpha$  and hv for PMMA/PbO(NPS) composites is illustrated in Figure 5. From the figure, straight lines

## Full Paper

TABLE 3 : The color parameters and their percentage changes for PMMA/PbO(NPS) composites

Color parameters	PMMA/PbO(NPS) composite (wt/wt%)				
	100.00/0.00	99.74/0.26	99.48/0.52	99.22/0.78	99.00/1.00
L	89.18	87.32	80.23	75.74	70.94
$\Delta L\%$	-	-2.09	-10.03	-15.07	-21.24
a	0.44	0.60	0.89	1.43	2.05
$\Delta a^*\%$	-	36.36	102.27	225.00	365.91
b	2.55	2.81	4.02	4.13	4.91
$\Delta b^*\%$	-	10.20	57.65	61.96	92.55
W	62.40	59.00	36.10	26.90	13.90
$\Delta W\%$	-	-5.45	42.15	56.89	77.72
$\Delta E$	-	1.87	9.08	13.57	18.46
$\Delta C$	-	2.48	4.12	4.37	5.32
$\Delta H$	-	75.91	77.49	70.93	67.37

Figure 4 : The absorption coefficient ( $\alpha$ ) as functions of wavelength (a) and photon energy (b) for PMMA/PbO(NPS) composites

were obtained and suggested that the absorption follows the quadratic relation for inter-band transitions and Urbach rule was verified<sup>[37]</sup>. The values of band tail energy ( $E_b$ ) were deduced from the slopes of these straight lines and their percentage changes were tabulated in TABLE 4. It is noticed that,  $E_b$  values decrease by increasing the concentration of PbO NPs up to 1.00 wt% (about 24.5%). These changes may be attributed to the variation in the internal fields associated with structure disorder in the PMMA

matrix<sup>[37]</sup>.

According to Tauc's model for higher values of absorption coefficient where the absorption was associated with inter-band transitions, it yields the power part which belongs to the Tauc<sup>[38]</sup> and Mott & Davis<sup>[37]</sup> formula as:

$$\alpha h\nu = B (h\nu - E_g)^n \quad (4)$$

where B is the slope of Tauc's edge called the band tail parameter in the range from  $1 \times 10^5$  to  $1 \times 10^6$  (cm.eV)<sup>-1</sup> and n is assumed to be 1/2 or 2 for al-

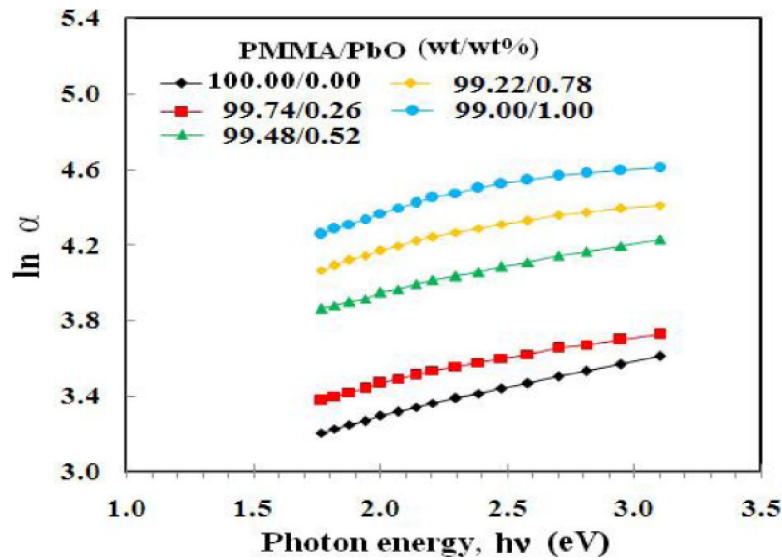
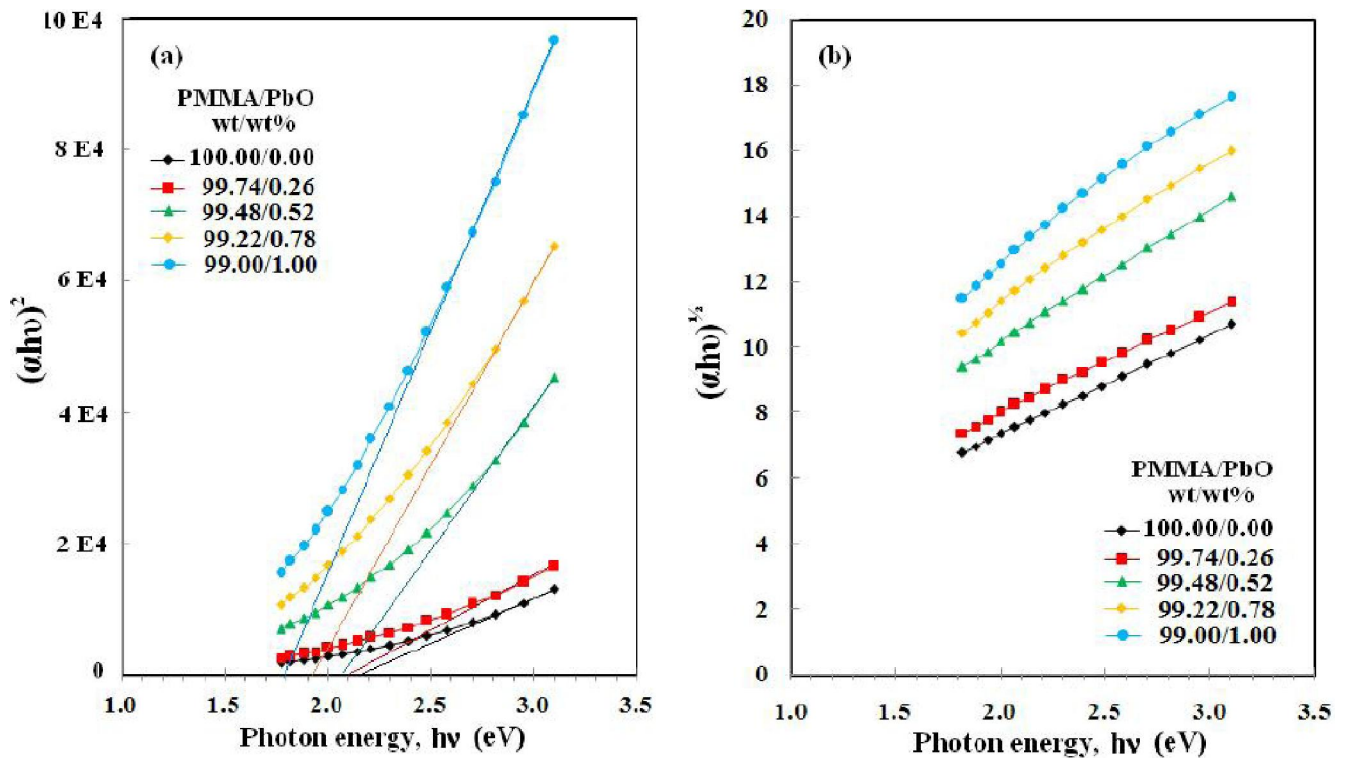


Figure 5 : Urbach law plots for PMMA/PbO(NPS) composites

TABLE 4 : Values of absorption coefficient ( $\alpha$ ) at 560 nm, band tail energy ( $E_b$ ), and direct energy gap ( $E_d$ ), and their percentage changes for PMMA/PbO(NPS) composites

PMMA/PbO(NPS) composite (wt/wt%)	$\alpha$ ( $\text{cm}^{-1}$ ) at 560 nm	$\Delta\alpha\%$	$E_b$ (eV)	$\Delta E_b\%$	$E_d$ (eV)	$\Delta E_d\%$
100.00/0.00	28.94	-	0.2842	-	2.168	-
99.74/0.26	34.38	18.80	0.2288	-19.49	2.110	-3.48
99.48/0.52	55.44	91.57	0.2279	-19.81	2.078	-4.94
99.22/0.78	69.80	141.19	0.2196	-22.73	1.923	-12.03
99.00/1.00	85.76	196.34	0.2146	-24.49	1.794	-17.93

Figure 6 : The variations of  $(\alpha h\nu)^2$  (a) and  $(\alpha h\nu)^{1/2}$  as functions of photon energy ( $h\nu$ ) for PMMA/PbO(NPS) composites

## Full Paper

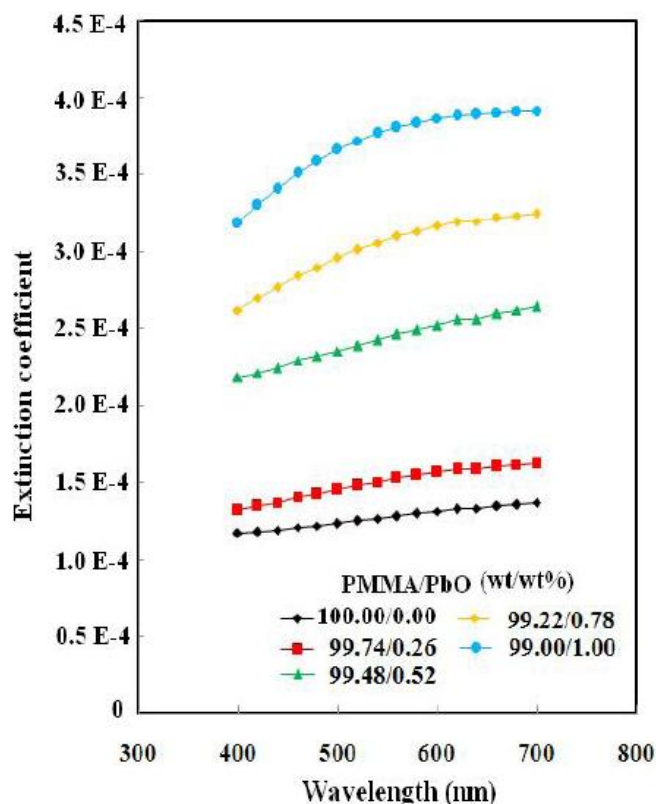


Figure 7 : Variation in the extinction coefficient ( $K$ ) as a function of wavelength for PMMA/PbO(NPS) composites

lowed direct and allowed indirect transitions, respectively, which represents the electronic transition responsible type for absorption. Figure 6a shows the variation of  $(\alpha h\nu)^2$  for PMMA/PbO(NPS) composites as a function of  $(h\nu)$ . The values of allowed direct energy gap ( $E_d$ ) were calculated by extending the linear parts of the curves to zero absorption and were represented in TABLE 4. It is observed that,  $E_d$  values decrease with increasing PbO NPs content up to 1.00 wt% by about 18% which indicates that the values of  $E_d$  show the dependence on the composition of the composite and creation of localized states in the band gap as a result of existence of PbO NPs. The variation of  $(\alpha h\nu)^{1/2}$  as a function of  $h\nu$  were shown in Figure 6b. It may be presumed that the obtained changes may be due to the change in molecular configuration induced by PbO NPs content<sup>[32-34]</sup>. It is noticed that the decrease in the values of  $E_b$  and  $E_d$  with increasing the concentration of PbO NPs may be due to that PbO NPs induced structural changes in the system. On other hand, these decreases may arise from the random

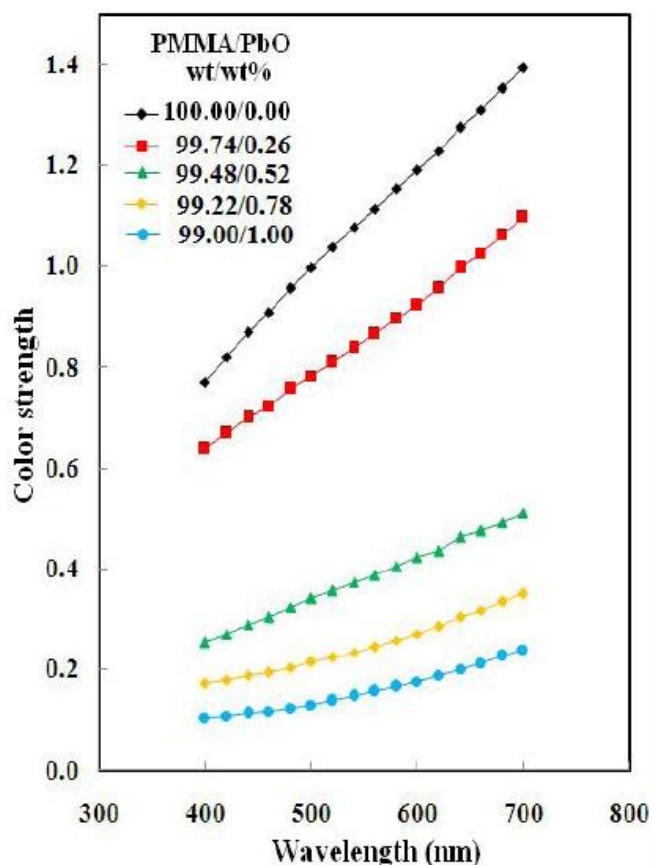


Figure 8 : Variation in the color strength ( $\alpha/S$ ) as a function of wavelength for PMMA/PbO(NPS) composites

fluctuations of the internal fields associated with the structure disorder in the amorphous region of the polymer material<sup>[32]</sup> (PMMA).

The extinction coefficient ( $K$ ) was a parameter characterizing the photonic material and was calculated from the transmittance spectra using the equation<sup>[36]</sup>:

$$K = \alpha\lambda/4\pi \quad (5)$$

$\lambda$  is the wavelength (cm) and  $\alpha$  is the absorption coefficient ( $\text{cm}^{-1}$ ). The extinction coefficient ( $K$ ) describes the properties of the material to light of a given wavelength and indicates the amount of absorption loss when the electromagnetic wave propagates through the material. Figure 7 represents the variation in the extinction coefficient as a function of wavelength for PMMA/PbO(NPS) composites films. It is clear from the figure that the values of  $K$  were found to be small in the order  $10^{-4}$ . This indicates that the prepared composites were considered to be insulating materials at room temperature<sup>[39]</sup>. In addition, the increase in the extinction coefficient

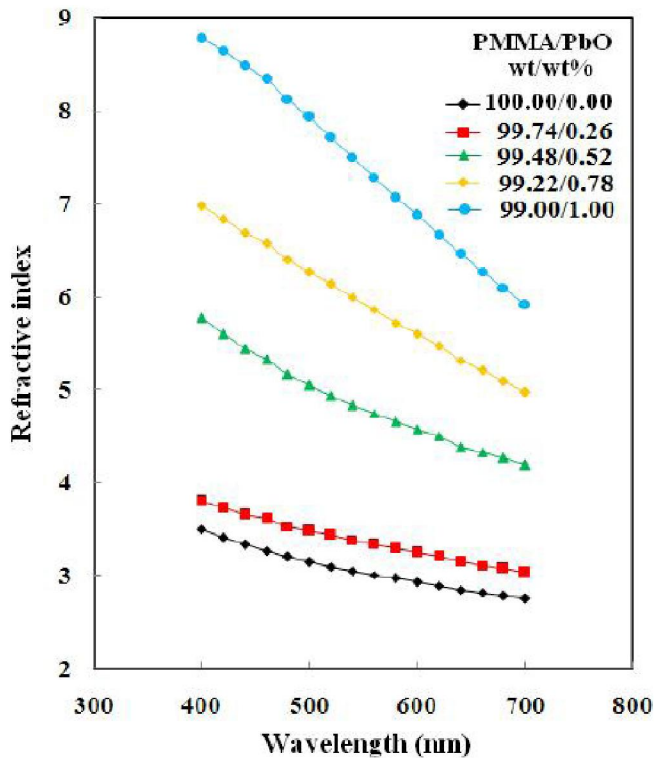


**Figure 9 :** The variation of refractive index ( $n$ ) as a function of wavelength ( $\lambda$ ) for PMMA/PbO(NPS) composites

values with increasing the wavelength and PbO Nps content shows that the fraction of light lost due to scattering.

Color strength ( $\alpha/S$ ) value has a close relationship to the amount of PbO NPs presented with PMMA network. The color strength of the prepared films was determined using Kubelka-Munk equation<sup>[40]</sup>:

$$\alpha/S = (1 - R)^2 / 2 R \quad (6)$$

$\alpha$  is the absorption coefficient and  $S$  is the scattering coefficient. Figure 8 shows the variation in the color strength ( $\alpha/S$ ) as a function of wavelength for PMMA/PbO(NPS) composites. It is clear from the figure that the values of  $\alpha/S$  increase with increasing wavelength and decrease markedly by increasing PbO NPs content. The decrease in  $\alpha/S$  values may be attributed the fact that PbO NPs give a fade color which is in agreement with the data of the color parameters.

The reflectance ( $R$ ) and the extinction coefficient ( $K$ ) data were used to determine the refractive index ( $n$ ) and some dispersion parameters. The refractive index ( $n$ ) of the prepared films was calcu-

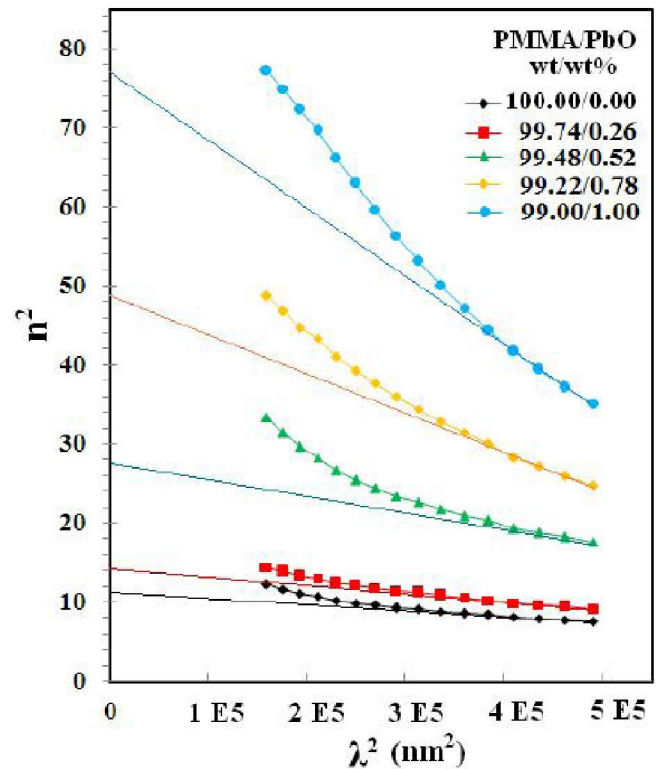


**Figure 10 :** The dependence of  $n^2$  on  $\lambda^2$  for PMMA/PbO(NPS) composites

lated according to the relation<sup>[44]</sup>:

$$n = [(1 + R)/(1 - R)] + \{[4R/(1 - R)^2] - K^2\}^{1/2} \quad (7)$$

where  $n$  is the real part of the complex refractive index given by  $\tilde{n} = n + ik$ . Figure 9 shows the refractive index distributions of PMMA/PbO(NPS) composites films in the visible region. The figure reveals that the values of  $n$  of the composite films increased markedly upon incorporation of PbO NPs into the PMMA matrix. Also,  $n$  values decrease with increasing the wavelength ( $\lambda$ ). The increased in the values of  $n$  by increasing PbO NPs content may be caused when the incident light interacts with the material that has a large amount of particles, the refraction will be higher and hence the refractivity of the films will increase<sup>[27]</sup>. Such increases in  $n$  may allow these materials to be used as an anti-reflection coating for solar cells, or as high-refractive index lenses.

The lattice dielectric constant ( $\epsilon_1$ ) and the ratio of carrier concentration to electron effective mass ( $e^2N/\pi c^2 m^*$ ) can be calculated by plotting the variation of  $n^2$  versus  $\lambda^2$  and according to the dispersion relation<sup>[42]</sup>:

## Full Paper

**TABLE 5 :** Values of  $\epsilon_1$ , ( $e^2N/\pi c^2m^*$ ), the energy parameter ( $E_p$ ), the single oscillator energy ( $E_o$ ), the long-wavelength refractive index ( $n_\infty$ ),  $\lambda_o$  is the average inter-band oscillator wavelength ( $\lambda_o$ ) and the average oscillator strength ( $S_o$ ) and their percentage changes for PMMA/PbO(NPS) composites

Dispersion parameters	PMMA/PbO(NPS) composite (wt/wt%)				
	100.00/0.00	99.74/0.26	99.48/0.52	99.22/0.78	99.00/1.00
$\epsilon_1$	11.167	14.105	27.616	48.350	77.373
$\Delta\epsilon_1\%$	-	26.31	147.30	332.97	592.87
$(e^2N/\pi c^2m^*) \times 10^{-6}$	7.299	10.098	20.408	48.449	86.637
$\Delta(e^2N/\pi c^2m^*)\%$	-	38.35	179.60	563.78	1086.97
$E_p$ (eV)	4.811	4.964	5.072	5.248	5.554
$\Delta E_d\%$	-	3.12	5.43	9.08	15.44
$E_o$ (eV)	31.931	47.344	89.651	163.540	292.771
$\Delta E_o\%$	-	48.27	180.76	412.17	816.89
$n_\infty$	2.763	3.246	4.321	5.671	7.329
$\Delta n_\infty\%$	-	17.48	56.39	105.25	165.26
$\lambda_o$ (nm)	258	250	240	236	223
$\Delta\lambda_o\%$	-	-3.10	6.98	8.53	13.57
$S_o$ ( $nm^{-2}$ ) $\times 10^{-4}$	0.999	1.528	3.077	5.592	10.578
$\Delta S_o\%$	-	52.95	208.01	459.76	958.86

$$n^2 = \epsilon_1 - (e^2N/\pi c^2m^*) \lambda^2 \quad (8)$$

The variation of  $n^2$  as a function of  $\lambda^2$  for PMMA/PbO(NPs) composites was shown in Figure 10. From the figure, the values of  $\epsilon_1$  and ( $e^2N/\pi c^2m^*$ ) were obtained from the intercept and the slope of the straight line parts. TABLE 5 reveals that the values of ( $e^2N/\pi c^2m^*$ ) increase with increasing PbO NPs content. This means that PbO NPS incorporation increases the charge carrier concentration inside the PMMA matrix.

From the dispersion behavior of refractive index ( $n$ ) and wavelength ( $\lambda$ ), different dispersion parameters can be deduced within the reflectance in the range 400–700 nm on the basis of the model reported by Wemple and DiDomenico<sup>[43]</sup>:

$$n^2 = 1 + [(E_p E_o)/(E_o^2 - hv)]^2 \quad (9)$$

$E_p$  is the energy parameter (a measure of the strength of inter-band optical transitions) and  $E_o$  is the single oscillator energy (the average excitation energy for electronic transitions).  $E_p$  and  $E_o$  were obtained from the intercept and slope of the linear part of  $(n^2-1)^{-1}$  and  $(hv)^2$  as depicted in Figure 11(a) and were tabulated in TABLE 5.

The change of  $n$  with  $\lambda$  can also be expressed by the dispersion equation as<sup>[44]</sup>:

$$(n_\infty^2 - 1)/(n^2 - 1) = 1 - (\lambda_o/\lambda)^2 \quad (10)$$

where  $n_\infty$  is the long-wavelength refractive index and  $\lambda_o$  is the average inter-band oscillator wavelength.

The average oscillator strength ( $S_o$ ) [ $= (n_\infty^2 - 1)/\lambda_o^2$ ] was also calculated. The parameters  $n_\infty$ ,  $\lambda_o$ , and  $S_o$  were obtained from the intercept and the slope of  $(n^2 - 1)^{-1}$  versus  $\lambda^{-2}$  curves (Figure 11b). The values of these parameters were given in TABLE 5. It was noticed that the dispersion parameters of PMMA were changed by the incorporation of PbO NPs into the PMMA matrix. This suggests that the optical constants of the prepared composites could be controlled by PbO NPs content. The quantitative measurements of these parameters may assist in tailoring and modeling the properties of such nanocomposites for use in optical components and devices.

The frequency dependence of the optical dielectric constant is a parameter that gives information about the electronic excitations inside the materials. The real ( $\epsilon_{real}$ ) and imaginary ( $\epsilon_{imag}$ ) parts of complex dielectric constants can be calculated by using the following relations<sup>[44]</sup>:

$$\epsilon_{real} = n^2(\lambda) - K^2(\lambda) \quad (11)$$

and

$$\epsilon_{imag} = 2 n(\lambda) K(\lambda) \quad (12)$$

Figure 12 shows the variation in the real value,  $\epsilon_{real}$  (a) and the imaginary value,  $\epsilon_{imag}$  (b) of the optical dielectric constant with photon energy ( $h\nu$ ) for PMMA/PbO(NPS) composites. It is clear from the figure that the values of  $\epsilon_{real}$  and  $\epsilon_{imag}$  increase with increasing PbO NPs content which may be attrib-

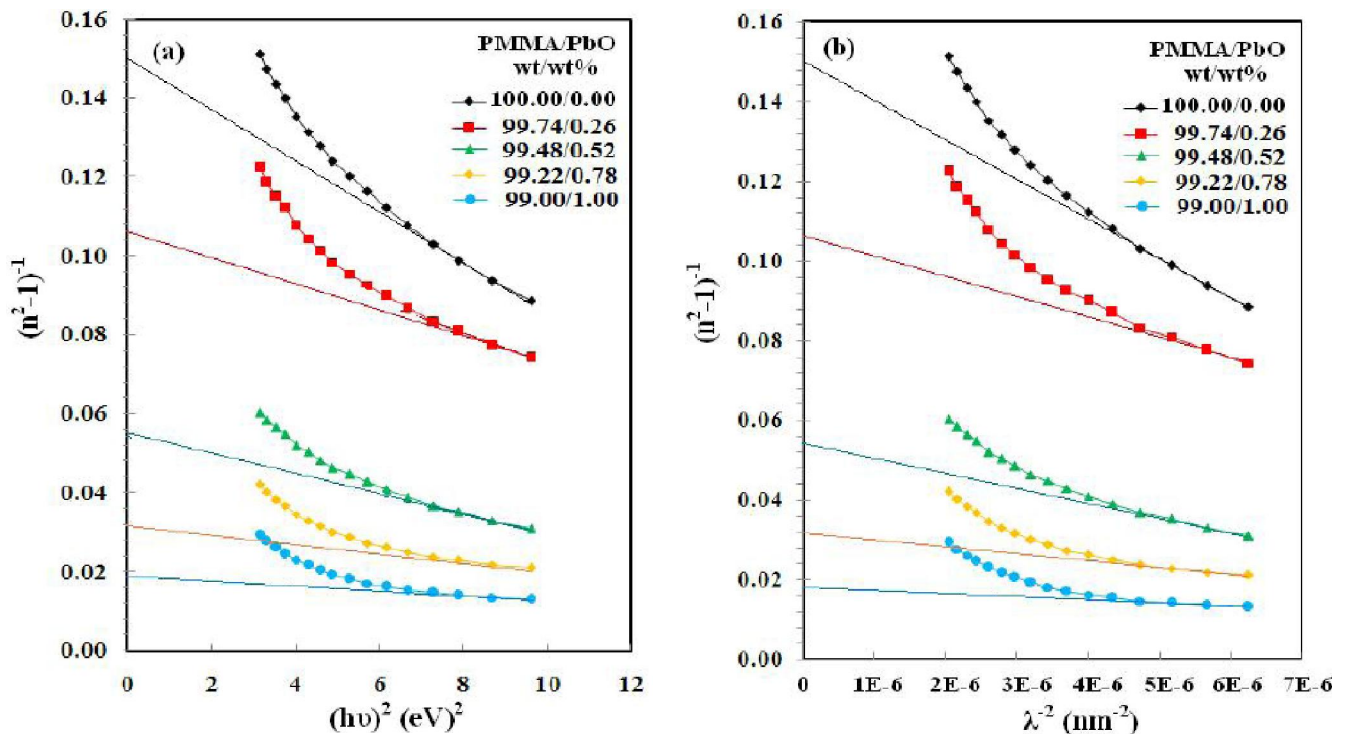


Figure 11 : The variation of  $(n^2-1)^{-1}$  as a function of  $(hv)^2$  (eV)<sup>2</sup> (a) and  $\lambda^{-2}$  (b) for PMMA/PbO(NPS) composites

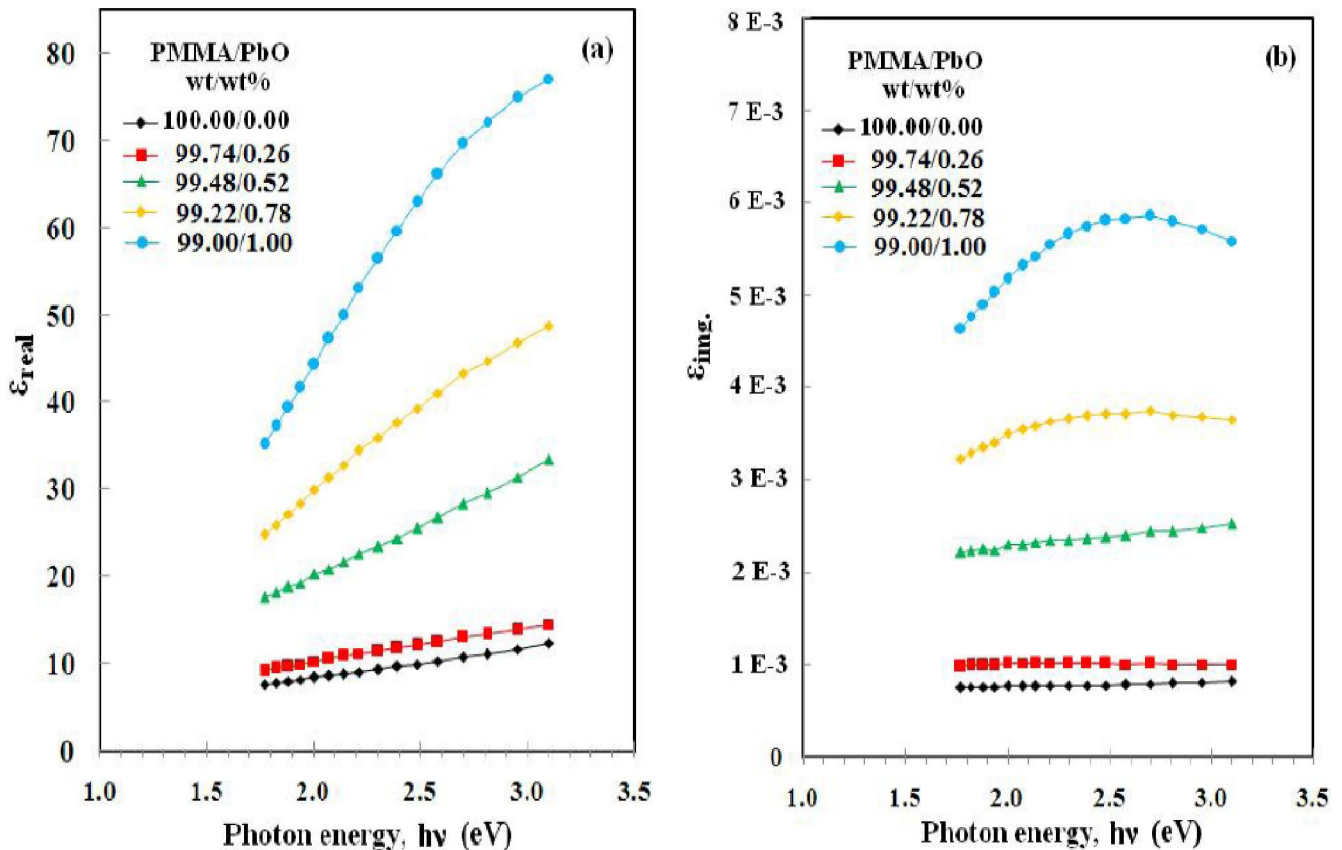


Figure 12 : The variation in the real value,  $\epsilon_{\text{real}}$  (a) and the imaginary value,  $\epsilon_{\text{img}}$  (b) of the optical dielectric constant as functions of photon energy ( $h\nu$ ) for PMMA/PbO(NPS) composites

uted to the high dielectric constant of PbO nanoparticles.

## CONCLUSIONS

The observed changes in the color parameters calculated from the transmittance spectra with increasing the concentration of PbO nanoparticles may be due to the changes produced in the physical bonds and in the molecular configuration of PMMA. These variations may lead to formation of new dopant centers of the polymeric material. In addition, the obtained data results of the optical (color and dispersion) parameters are of great importance for the improvement of the optical properties of the PMMA.

## REFERENCES

- [1] Salavati M.Niasari, F.Mohandes, F.Davar; *Polyhedron*, **28**, 2263 (2009).
- [2] E.E.Ferg, T.Phangalala, T.Dyl; *J.Appl.Electrochem.*, **40**, 383 (2010).
- [3] S.Liu, Z.R.Tang, Y.Sun, J.C.Colmenares, Y.J.Xu; *Chem.Soc.Rev.*, **44**, 5053 (2015).
- [4] P.Nandy, P.Bandyopadhyaya, A.Deya, R.Basu, S.Das; *Current Applied Physics*, **14**, 1149 (2014).
- [5] S.Li, W.Yang, M.Chen, J.Gao, J.Kang, Y.Qi; *Mater.Chem.Phys.*, **90**, 262 (2015).
- [6] H.Karami, M.A.Karami, S.Haghdar; *Mater.Res.Bull.*, **43**, 3054 (2008).
- [7] H.Karami, M.A.Karami, S.Haghdar, A.Sadeghi, Mir R.Ghasemi, Mahdi S.Khani; *Mater.Chem.Phys.*, **108**, 337 (2008).
- [8] L.Li, X.Zhu, D.Yang, L.Gao, J.Liu, R.V.Kumar, J.Yang; *J.Hazard.Mater.*, **203**, 274 (2012).
- [9] El A.Sayed Abdo, M.A.M.Ali, M.R.Ismail; *Radiat.Phys.Chem.*, **66**, 185 (2003).
- [10] W.H.Zhong, G.Sui, S.Jana, J.Miller; *Compos.Sci.Technol.*, **69**, 2093 (2009).
- [11] N.Erdem, O.Baykara, M.Dogru, F.Kuluozturk; *Radiat.Phys.Chem.*, **79**, 917 (2010).
- [12] V.Harish, N.Nagauah, T.N.Prabhu, K.T.Varughese; *J.Appl.Polym.Sci.*, **117**, 3623 (2010).
- [13] Y.R.Uhm, J.Kim, S.Lee, J.Jeon, C.K.Rhee; *Ind.Eng.Chem.Res.*, **50**, 4478 (2011).
- [14] B.Jia, L.Gao; *L.Mater.Chem.Phys.*, **100**, 351 (2006).
- [15] E.Ozkaraoglu, I.Tunc, S.Suzer; *Polymer*, **50**, 462 (2009).
- [16] P.K.Khanna, N.Singh, S.Charan; *Materials letters*, **61**, 4725 (2007).
- [17] A.Singh, U.K.Kulkarni, C.Khan-Malek; *Microelectronic Engineering*, **88**, 939 (2011).
- [18] K.Matsuyama, K.Mishima; *Journal of Supercritical Fluids*, **49**, 256 (2009).
- [19] J.C.K.Lai, M.B.Lai, S.Jandhyam, V.V.Dukhande, A.Bhushan, C.K.Daniels, S.W.Leung; *International Journal of Nanomedicine*, **3**, 533 (2008).
- [20] W.Ma, J.Zhang, X.Wang, S.Wang; *Applied Surface Science*, **253**, 8377 (2007).
- [21] C.Wochnowski, S.Metev, G.Sepold; *Applied Surface Science*, **706**, 154-155 (2000).
- [22] A.Silva, K.Dahmouche, B.Soaes; *Applied Clay Science*, **47**, 414 (2010).
- [23] V.L.Schade, T.S.Roukis; *Journal of Foot and Ankle Surgery*, **49**, 55 (2010).
- [24] S.P.Mohanty, M.N.Kumar, N.S.Murthy; *Journal of Orthopaedic Surgery*, **11**, 73 (2003).
- [25] N.L.Pleshko, A.L.Boskey, R.Mendelsohn; *Journal of Histochemistry and Cytochemistry*, **40**, 1413 (1992).
- [26] A.Stevens, J.Germain; '*Resin Embedding Media*', J.D.Bancroft, A.Stevens (Editors), The theory and practice of histological techniques, 3<sup>rd</sup> Edition, New York, Churchill Livingstone, (1990).
- [27] A.M.El Sayed, W.M.Morsi; *Polym.Compos.*, **34**, 2031 (2013).
- [28] A.M.El Sayed, W.M.Morsi; *J.Mater.Sci.*, **49**, 5378 (2014).
- [29] A.Hassen, S.El-Sayed, W.M.Morsi, A.M.El Sayed; *Journal of Advances in Physics*, **4**, 571 (2014).
- [30] CIE Recommendation on Colorimetry; CIE Publ.No.15.2.Central Bureau of the CIE, Vienna, (1986).
- [31] CIE Recommendation on Uniform Color Spaces; Color Difference Equations, Psychometric Color Terms, Suppl.No.2 of CIE Publ.No.15 (E-1.3.1), Paris, (1971;1978).
- [32] O.W.Guirguis, M.T.H.Moselhey; *J.Mater.Sci.*, **46**, 5775 (2011).
- [33] A.B.P.Lever; '*Organic Electronic Spectroscopy*', Elsevier, Amsterdam, Netherland, (1968).
- [34] A.Miller; '*Handbook of Optics*', McGraw-Hill, New York, USA, **1**, (1994).
- [35] A.A.Maradulin, E.W.Montroll, G.H.Weiss; '*Theory of lattice dynamics in the harmonic approximation*', Academic Press, New York, USA, (1963).
- [36] R.Tintu, K.Saurav, K.Sulakshna, V.P.N.Nampoori, P.Radhakrishnan, S.Thomas; *Journal of Non-Oxide Glasses*, **2**, 167 (2010).
- [37] N.F.Mott, E.A.Davis; '*Electronic processes in non-crystalline materials*', Oxford: Clarendon, (1979).

- [38] D.L.Wood, J.Tauc; Phys.Rev.B, **5**, 3144 (1972).      [42] R.P.Chahal, S.Mahendia, A.K.Tomar, S.Kumar; Journal of Alloys and Compounds, **538**, 212 (2012).
- [39] J.I.Pankove; 'Optical Process in semiconductors', Devers Publication, New York, USA, (1975).      [43] S.H.Wemple, M.DiDomenico Jr; Phys.Rev.B, **3**, 1338 (1970).
- [40] D.B.Judd, G.Wyszecki; 'Color in business science and industry', 3<sup>rd</sup> Edition, John Wiley & Sons, Inc.New York, (1975).      [44] A.A.Al-Ghamdi; Vacuum, **80**, 400 (2006).
- [41] A.M.El Sayed, H.M.Diab, R.El Mallawany; J.Polym.Res., **20**, 1 (2013).